An Evaluation of Particle Filter on Contact-SLAM Problems

Shuai Li, Siwei Lyu*, Jeff Trinkle, and Wolfram Burgard**
Department of Computer Science, Rensselaer Polytechnic Institute
Department of Computer Science, University at Albany, SUNY*
Department of Computer Science, University of Freiburg**

Introduction

The contact-SLAM problem or C-SLAM problem is a broad class of grasping and manipulation problem and it is very important to robotic manipulation tasks.

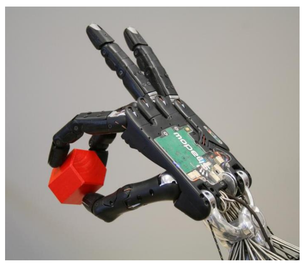

Figure 1: Robot hand manipulation.

We focus on understanding fundamental modeling choices through analysis of real and simulated experiments. We compare the results of both rigid body and compliant body model with several sources of noise to better understand relevant aspects of the implementation of particle filters for C-SLAM problems.

Dynamic Models

We study object tracking and the identification of the binary contact state and consider the case where a robot arm is moving into contact with an object.

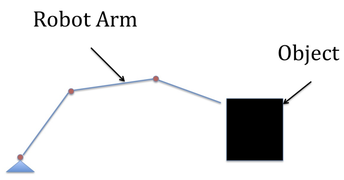

Figure 2: Robot arm moving into contact with an object.

The dynamics of the arm and object expressed in the workspace:

$$\tilde{M}(\theta)\ddot{x} = \tilde{J}^T\lambda + \tilde{D}(\theta,\dot{\theta})$$
$$0 \le \lambda \perp \Psi(x) \ge 0$$

Rigid Body Model

The rigid body model can be described by a LCP as follows

$$\begin{aligned} mv_{t+1} &= u_t h - \lambda_{t+1} h + mv_t \\ x_{t+1} &= v_{t+1} h + x_t \\ \Psi_{t+1} &= x_{\text{wall}} - x_{t+1} \\ 0 \le \lambda_{t+1} &\perp \Psi_{t+1} \ge 0 \end{aligned}$$

Compliant Body Model

Replace the complementarity condition by the following equations

$$\begin{aligned} \delta_t &= max\{0, -\Psi_t\} \\ \dot{\delta}_t &= \frac{1}{h}\left[max\{0,-\Psi_t\} - max\{0,-\Psi_{t-1}\}\right] \\ \lambda_{t+1} &= max\{0, K\delta_t + C\dot{\delta}_t\} \end{aligned}$$

Filtering Mothods

We use a SIR particle fitler combined with two probabilistic models, which are adding noise to the input forces and the state vector. We also introduce two additional filtering method to deal with the complimentarity condition and noisy F/T sensor readings.

Algorithm 1 SIR Particle Filter Update State

function UPDATE_STATE(Z_t, u_t, N, w_t)
  for $i = 1 \to N$ **do**
    $\bar{Z}_{t+1}^{[i]} = State\ Transit(Z_t^{[i]}, u_t)$
    $\bar{w}_{t+1}^{[i]} = P(o_{t+1} \mid \bar{Z}_{t+1}^{[i]}) \cdot w_t^{[i]}$
  end for
  Normalize $\bar{w}_{t+1}$
  return $\bar{Z}_{t+1}$, $\bar{w}_{t+1}$
end function

- *noisy input particle filter (NIPF)* Adds a white Gaussian noise to the input force before state transition.
- *noisy state particle filter (NSPF)* Adds a white Gaussian noise to the states after state transition.
- *projected particle filter (PJPF)* Adds additional weights to the particles according to their projected distances to the complementarity condition plane.
- *force state particle filter (FSPF)* Makes input force as a state and observe F/T sensor reading.

Acknowledgement

- This work is supported by NSF under grant number IIS-1208468 (National Robot Initiative).

Experiments

We perform both virtual and physical experiments.

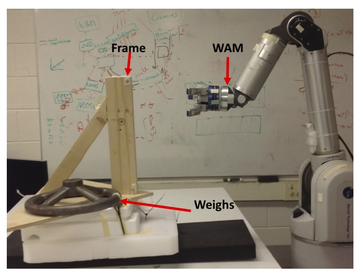

Figure 3: Physical Experiment.

For the physical experiments, we use a Barrett WAM whose palm moves into contact with a stiff wall under guarded control. The F/T sensor at the wrist of the robot arm is used to read the forces on the palm. For the virtual experiments, the WAM is modeled as a rigid block moved by an external force towards a rigid wall.

Results

We divided the estimation task into two stages: robot tracking and contact prediction. During the tracking stage (prior to contact), the dynamic models are linear, so the particle filters were compared to each other and to Kalman filters. For the contact prediction stage, contact confidence (the sum of the weights of the particles that are in contact) was used as the performance criterion.

Tracking Results

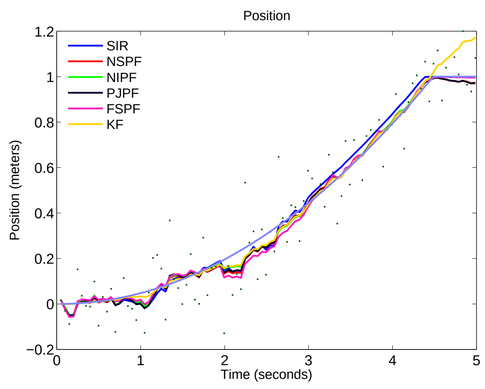

Figure 4: Tracking of the position, virtual experiment.

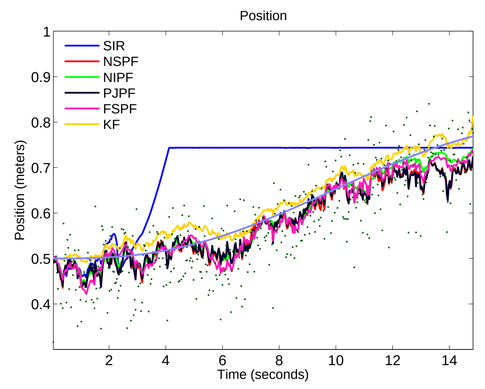

Figure 5: Tracking of the position, physical experiment.

Contact Prediction Results

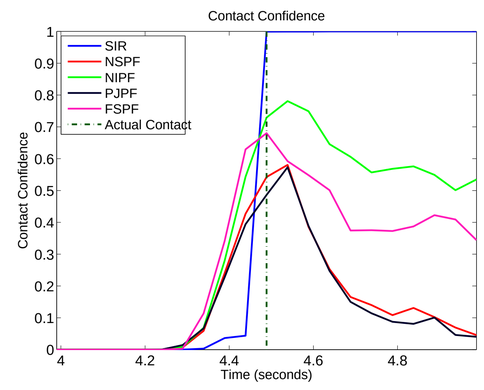

Figure 6: Contact prediction, rigid body model, virtual experiment.

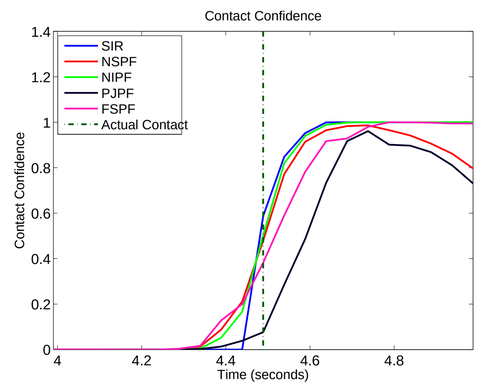

Figure 7: Contact prediction, compliant body model, virtual experiment.

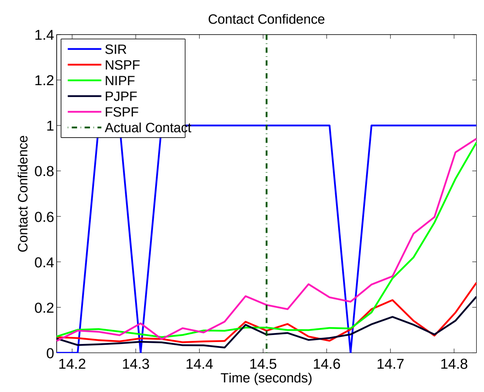

Figure 8: Contact prediction, rigid body model, physical experiment.

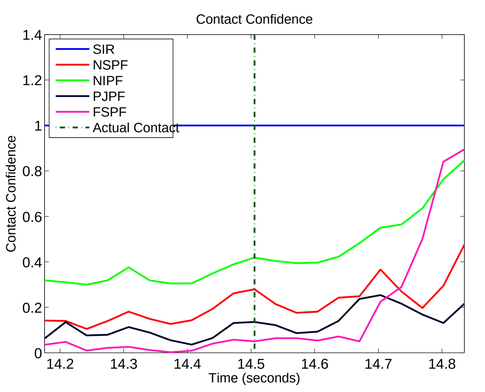

Figure 9: Contact prediction, compliant body model, physical experiment.